ductive and nonreproductive tissues alike. Deficiency of androgens (and probably estrogens) in males, due to castration or a decline in production with old age, is a major factor in the development of osteoporosis in men as well (*19*, *20*).

The benefits of sex steroid replacement during late postreproductive life derive primarily from the actions of sex steroids on nonreproductive tissues, whereas its side effects result from actions on reproductive tissues. The favorable effects of estren on bone and its lack of effect on reproductive tissues indicate that mechanism-specific ligands may offer advantages over estrogens or SERMs (*21*, *22*) in the setting of hormone replacement therapy. Growing concern about the efficacy and safety of existing hormone replacement therapies (*23*, *24*) makes these new ideas timely.

References and Notes

1. J. G. Moggs, G. Orphanides, *EMBO Rep.* **2**, 775 (2001).
2. N. J. McKenna, B. W. O'Malley, *Cell* **108**, 465 (2002).
3. B. S. McEwen, S. E. Alves, *Endocr. Rev.* **20**, 279 (1999).
4. E. Falkenstein, H. C. Tillmann, M. Christ, M. Feuring, M. Wehling, *Pharmacol. Rev.* **52**, 513 (2000).
5. S. Kousteni *et al.*, *Cell* **104**, 719 (2001).
6. S. Kousteni *et al.*, *J. Bone Miner. Res.* **17**, S169 (2002).
7. Materials and Methods are available as supporting material on *Science* Online.
8. A. Samuels, M. J. Perry, J. H. Tobias, *J. Bone Miner. Res.* **14**, 178 (1999).
9. A. T. Mancino *et al.*, data not shown.
10. S. C. Manolagas, S. Kousteni, *Endocrinology* **142**, 2200 (2001).
11. Z. Chen *et al.*, *J. Clin. Invest.* **103**, 401 (1999).
12. T. De Jager *et al.*, *J. Biol. Chem.* **276**, 27873 (2001).
13. J. L. Fitzpatrick *et al.*, *J. Neurochem.* **82**, 674 (2002).
14. H. M. Reichardt *et al.*, *Cell* **93**, 531 (1998).
15. P. J. Kushner *et al.*, *J. Steroid Biochem. Mol. Biol.* **74**, 311 (2000).
16. L. Grotewold, U. Rüther, *EMBO J.* **21**, 966 (2002).
17. L. M. Boyden *et al.*, *N. Engl. J. Med.* **346**, 1513 (2002).
18. S. C. Manolagas, *Endocr. Rev.* **21**, 115 (2000).
19. ———, S. Kousteni, R. L. Jilka, *Recent Prog. Horm. Res.* **57**, 385 (2002).
20. B. L. Riggs, S. Khosla, L. J. Melton III, *Endocr. Rev.* **23**, 279 (2002).
21. P. M. Doran, B. L. Riggs, E. J. Atkinson, S. Khosla, *J. Bone Miner. Res.* **16**, 2118 (2001).
22. S. M. Ott, A. Oleksik, Y. Lu, K. Harper, P. Lips, *J. Bone Miner. Res.* **17**, 341 (2002).
23. L. Mosca *et al.*, *Circulation* **104**, 499 (2001).
24. Writing Group for the Women's Health Initiative Investigators, *JAMA* **288**, 321 (2002).

25. We thank B. S. and J. A. Katzenellenbogen for pyrazole, experimental assistance, and critical comments on the manuscript; P. K. Roberson and S. Korourian for expert advice; V. Lowe, R. Shelton, and J. Crawford for technical assistance; and M. Douglas for preparation of the manuscript. Supported by grants from NIH (P01-AG13918 to S.C.M. and KO2-AR02127 to T.B.); the Department of Veterans Affairs (merit and REAP awards to S.C.M.); and Anabonix Inc. (Little Rock, AR), which has a licensing agreement with the University of Arkansas for Medical Sciences to develop and commercialize anabolic drugs for osteoporosis, including the prototypic ligand described in this manuscript.

Supporting Online Material

www.sciencemag.org/cgi/content/full/298/5594/843/DC1
Materials and Methods
Figs. S1 to S3
Table S1
References and Notes

11 June 2002; accepted 4 September 2002

Treatment of Ischemic Brain Damage by Perturbing NMDA Receptor–PSD-95 Protein Interactions

Michelle Aarts,[1]* Yitao Liu,[2,3,4]* Lidong Liu,[2,3,4] Shintaro Besshoh,[5] Mark Arundine,[1] James W. Gurd,[5] Yu-Tian Wang,[2,3,4] Michael W. Salter,[3,6]† Michael Tymianski[1,6,7]†

***N*-methyl-D-aspartate receptors (NMDARs) mediate ischemic brain damage but also mediate essential neuronal excitation. To treat stroke without blocking NMDARs, we transduced neurons with peptides that disrupted the interaction of NMDARs with the postsynaptic density protein PSD-95. This procedure dissociated NMDARs from downstream neurotoxic signaling without blocking synaptic activity or calcium influx. The peptides, when applied either before or 1 hour after an insult, protected cultured neurons from excitotoxicity, reduced focal ischemic brain damage in rats, and improved their neurological function. This approach circumvents the negative consequences associated with blocking NMDARs and may constitute a practical stroke therapy.**

Protein-protein interactions govern signals involved in cell growth, differentiation, and intercellular communication through dynamic associations between modular protein domains and their cognate binding partners (*1*). At excitatory synapses of central neurons, ionotropic glutamate receptors are organized into multiprotein signaling complexes within the postsynaptic density (PSD) (*2*). A prominent organizing protein is PSD-95 (*3*), which couples the NMDAR to intracellular proteins and signaling enzymes (*2*, *4*). Through its second PDZ domain (PDZ2), PSD-95 binds the COOH-terminus tSXV motif of NMDAR NR2 subunits as well as neuronal nitric oxide synthase (nNOS) (*3*, *4*). This binding couples NMDAR activity to the production of nitric oxide (NO), a signaling molecule that mediates NMDAR-dependent excitotoxicity (*5*). NMDAR activity is unaffected by genetically disrupting PSD-95 in vivo (*6*) or by suppressing its expression in vitro (*7*). Nonetheless, PSD-95 deletion dissociates NMDAR activity from NO production and suppresses excitotoxicity (*7*).

Although NMDARs mediate ischemic brain injury (*8*), blocking them is deleterious to animals and humans (*9*–*11*). Targeting PSD-95 protein therefore represents an alternative therapeutic approach for diseases that involve excitotoxicity. Because mutation or suppression of PSD-95 is therapeutically impractical, we hypothesized that perturbing its interaction with NMDARs could suppress excitotoxicity and ischemic brain damage. This might be achieved by the intracellular introduction of peptides that bind to either the NR2 or the PDZ2 interaction domains (Fig. 1A). To bind PDZ2 domains, we constructed a peptide comprising the nine COOH-terminal residues of NR2B (Lys-Leu-Ser-Ser-Ile-Glu-Ser-Asp-Val; NR2B9c) (*3*). To bind NR2 subunits, we used residues 65 to 248 of PSD-95, encoding the first and second PDZ domains (PDZ1-2). NR2B9c and PDZ1-2 were rendered cell-permeant by fusing each to the cell-membrane transduction domain of the human immunodeficiency virus–type 1 (HIV-1) Tat protein (Tyr-Gly-Arg-Lys-Lys-Arg-Arg-Gln-Arg-Arg-Arg) (*12*) to obtain a 20–amino acid peptide (Tat-NR2B9c) and the fusion protein pTat-PDZ1-2, respectively (*13*).

First, we determined whether Tat-NR2B9c would transduce into neurons. The fluorophore dansyl chloride was conjugated to Tat-NR2B9c and to a control peptide comprising HIV-1 Tat residues 38 to 48 (Lys-Ala-Leu-Gly-Ile-Ser-Tyr-Gly-Arg-Lys-Lys; Tat38-48) outside the transduction domain (*14*). These were bath-applied to cultured cortical neurons and their fluorescence was visualized by confocal microscopy. Neurons treated with Tat-NR2B9c-dansyl (10 μM) exhibited fluorescence in their cytoplasm and processes, indicating intracellular peptide uptake (Fig. 1B, left), whereas cultures treated

[1]Toronto Western Hospital Research Institute, 11-416 MC-PAV, 399 Bathurst Street, Toronto, Ontario M5T 2S8, Canada. [2]Divisions of Laboratory Medicine and Pathobiology, [3]Programme in Brain and Behaviour, Hospital for Sick Children, 555 University Avenue, Toronto, Ontario M5G 1X8, Canada. [4]Brain Research Center and Department of Medicine, Vancouver Hospital and Health Sciences Center, University of British Columbia, Vancouver, British Columbia V6T 1Z3, Canada. [5]Centre for the Neurobiology of Stress, Division of Life Sciences, University of Toronto at Scarborough, Toronto, Ontario M1C 1A3, Canada. [6]Department of Physiology, [7]Department of Surgery, University of Toronto, Toronto, Ontario M5S 1A8, Canada.

*These authors contributed equally to this report.
†To whom correspondence should be addressed. E-mail: mike_t@uhnres.utoronto.ca, mike.salter@utoronto.ca

with Tat38-48-dansyl (10 μM), devoid of the transduction domain, exhibited only background signal indicating no peptide uptake (Fig. 1B, right). Tat-NR2B9c-dansyl accumulation was detectable in neurons within 10 min of application, peaked during the next 20 min, and remained detectable for 5 hours after washing the peptide from the bath (Fig. 1C).

Next we determined whether Tat-NR2B9c could perturb preformed NMDAR–PSD-95 complexes by examining its effects on the coimmunoprecipitation of PSD-95 with NR2 subunits (*13*). The P2 membrane protein fraction of rat forebrain tissue, which is enriched in synaptic structures, was incubated with Tat-NR2B9c or with one of three controls: Tat38-48, the Tat transduction sequence conjugated to two alanine residues (Tat-AA), or a Tat-NR2B9c peptide in which the COOH-terminal tSXV motif contained a double point mutation (Lys-Leu-Ser-Ser-Ile-Glu-Ala-Asp-Ala; Tat-NR2B-AA) rendering it incapable of binding PSD-95 (*3*). None of these controls, each lacking an intact PDZ binding motif, reduced the coimmunoprecipitation of PSD-95 with NR2B. However, Tat-NR2B9c, in which the Ile-Glu-Ser-Asp-Val sequence is preceded by residues unique to the NR2B COOH-terminus, selectively reduced the coimmunoprecipitation of PSD-95 with NR2B (Fig. 1D), but not with NR2A (Fig. 1E). Thus, NR2A may be more tightly bound to PSD-95. Alternatively, the incomplete homology of Tat-NR2B9c for the NR2A COOH-terminus may make it less effective in perturbing PSD-95–NR2A binding (*13*).

Because synaptic and whole-cell NMDAR currents are unaffected when PSD-95 is lacking (*6, 7*), we examined NMDAR currents and Ca^{2+} fluxes when PSD-95 is dissociated. Bath application of Tat-NR2B9c (50 nM) to acute rat hippocampal slices had no effect on synaptic responses of CA1 neurons evoked by stimulation of the Schaffer collateral-commissural pathway (Fig. 2A). Tat-NR2B9c also had no effect on patch recordings in CA1 neurons of the primarily AMPAR (AMPA receptor)–mediated total excitatory postsynaptic current (EPSC) (Fig. 2B) (*15*), nor on the isolated NMDA component of the EPSC (Fig. 2C) (*13*). Moreover, pretreating cultured cortical neurons with Tat-NR2B9c or with pTat-PDZ1-2 (each at 50 nM) did not alter $^{45}Ca^{2+}$ uptake produced by applying NMDA (Fig. 2D). The rate of rise and peak levels of free intracellular calcium concentration ($[Ca^{2+}]_i$) in response to NMDA were also unaffected by Tat-NR2B9c (*13, 16*). CNQX (6-cyano-7-nitroquinoxaline-2,3-dione; 10 μM) and nimodipine (2 μM) were present in the extracellular solution in these and all further experiments in cultures, so as to isolate signaling to NMDARs and prevent secondary activation of AMPARs or of voltage-gated Ca^{2+} channels, respectively (*7, 17, 18*).

We next determined whether Tat-NR2B9c affected signaling events downstream of NMDAR activation. NMDA-evoked changes in guanosine 3′,5′-monophosphate (cGMP) level were measured as a surrogate measure of NO production by nNOS (*7, 19*). We focused on nNOS activity because it mediates neurotoxic sequelae of NMDAR activation (*5*) and, along with other signaling molecules bound to

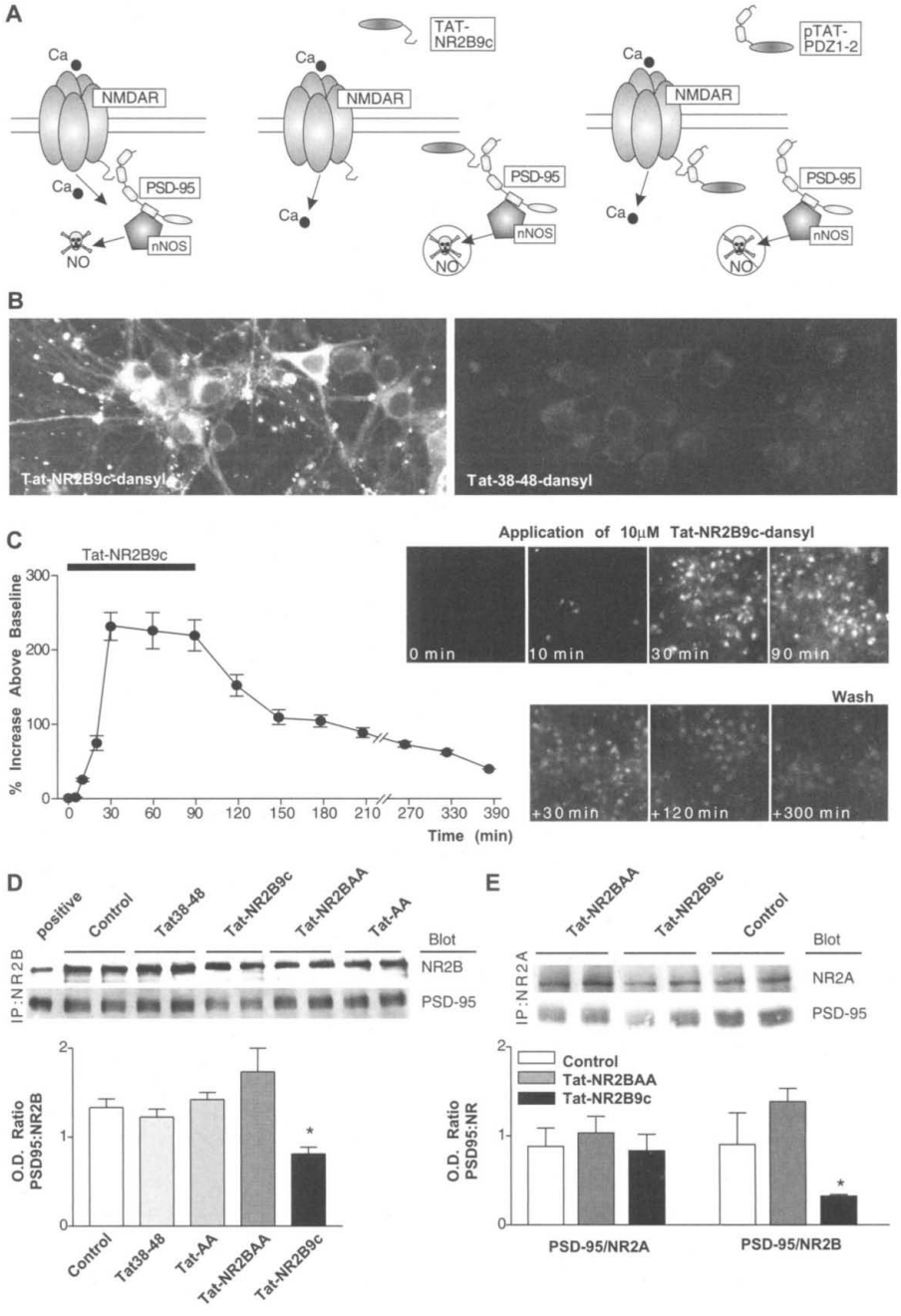

Fig. 1. Utility of Tat peptides in dissociating the NMDAR–PSD-95 interaction (**A**) The hypothesis: The NMDAR–PSD-95 complex (left panel) may be dissociated using Tat peptides fused either to the COOH-terminus of NR2B (Tat-NR2B9c; middle) or to the first and second PDZ domains of PSD-95 (pTat-PDZ1-2; right), thus reducing the efficiency of excitotoxic signaling. (**B**) Visualization of intraneuronal accumulation of Tat-NR2B9c-dansyl (10 μM) but not Tat38-48-dansyl (10 μM) 30 min after application to cortical cultures (excitation, 360 nm; emission, >510 nm; representative of five experiments). Fluorescence of cultures treated with Tat38-48-dansyl was similar to background. (**C**) Time course of Tat-NR2B9c-dansyl (10 μM) fluorescence after application to cortical cultures at room temperature (symbols: mean ± SE of four experiments). Inset: fluorescence images from a representative experiment. (**D** and **E**) Coimmunoprecipitation of PSD-95 with NR2 subunits in rat forebrain P2 membrane fractions treated with Tat peptides. (D) Tat-NR2B9c reduced the optical density (O.D.) ratio of PSD-95:NR2B by 37.6 ± 8.2% relative to controls. ANOVA, $F = 6.086$, $^*P = 0.0041$. (E) No significant effect on O.D. ratio of PSD-95:NR2A while reducing O.D. ratio of PSD-95:NR2B (ANOVA, $^*P < 0.01$) in same tissue extract. Top: Representative gels. Bottom: Means ± SE of four to eight experiments.

PSD-95, should be dissociated from NMDARs by Tat-NR2B9c. Cultured cortical neurons were pretreated with Tat-NR2B9c (50 nM), the noninteracting Tat-NR2B-AA (50 nM), or sham washes for 1 hour and then challenged with NMDA (0 to 1000 μM). NMDA produced a concentration-dependent increase in cGMP that was significantly suppressed (average of 39.5 ± 6.7%) by pretreating the cultures with Tat-NR2B9c, but not with Tat-NR2B-AA (Fig. 2E).

Although Tat-NR2B9c treatment did not affect NMDAR-mediated currents or Ca^{2+} fluxes, it interfered with NMDAR–PSD-95 binding and suppressed downstream NO signaling. Thus, we examined whether such treatment enhances neurons' resilience to NMDA toxicity. Cortical neuronal cultures were pretreated with sham washes, Tat-NR2B9c, or the noninteracting control Tat-NR2B-AA (each at 50 nM) for 1 hour, then exposed to NMDA (0 to 100 μM) for 1 hour followed by a 20-hour observation period (fig. S1, inset). Cell death at all NMDA concentrations was significantly reduced by Tat-NR2B9c pretreatment, whereas Tat-NR2B-AA was ineffective (fig. S1). Pretreatment with pTat-PDZ1-2 also attenuated NMDA neurotoxicity to a similar degree (fig. S1) (*13*), which suggested that targeting either side of the NMDAR–PSD-95 interaction (Fig. 1A) reduces excitotoxic damage.

Agents that block NMDAR activity are deleterious or ineffective in treating stroke in animals and humans (*9–11*). Because Tat-NR2B9c attenuates NMDA toxicity without blocking NMDARs, we reasoned that its application in the treatment of stroke would constitute an improvement over NMDAR blockers.

We first determined whether Tat-NR2B9c could be delivered into the brain in the intact animal. C57BL/6 mice (25 g) were injected intraperitoneally with a 500-μmol dose of either Tat-NR2B9c-dansyl or Tat38-48-dansyl as a cell-impermeant control. Coronal brain sections taken 1 hour after injection were examined by confocal microscopy for fluorescent peptide uptake (*13*). Brains from animals injected with Tat-NR2B9c, but not Tat38-48-dansyl, exhibited strong fluorescence in the cortex (fig. S2A) (*20*). Similar results were obtained with intravenous injection in rats (*21*), confirming that Tat-NR2B9c enters the brain upon peripheral administration.

Next, we examined whether pretreatment with Tat-NR2B9c would reduce stroke damage. Adult male Sprague-Dawley rats were subjected to transient middle cerebral artery occlusion (MCAO) for 90 min by the intraluminal suture method (*13, 22, 23*). Animals were pretreated by a single intravenous bolus injection with saline, the Tat-NR2B-AA control, or Tat-NR2B9c 45 min before MCAO (3 nmol/g). Body temperature, blood pressure, and blood gases were monitored and maintained throughout the experiment (table S1). The extent of cerebral infarction was measured 24 hours after MCAO onset (fig. S2C, inset). The postural reflex test (*24*) and the forelimb placing test (*25*) were used to grade neurological function on a scale of 0 to 12 (normal = 0; worst = 12) during MCAO (at 50 min) and 24 hours thereafter.

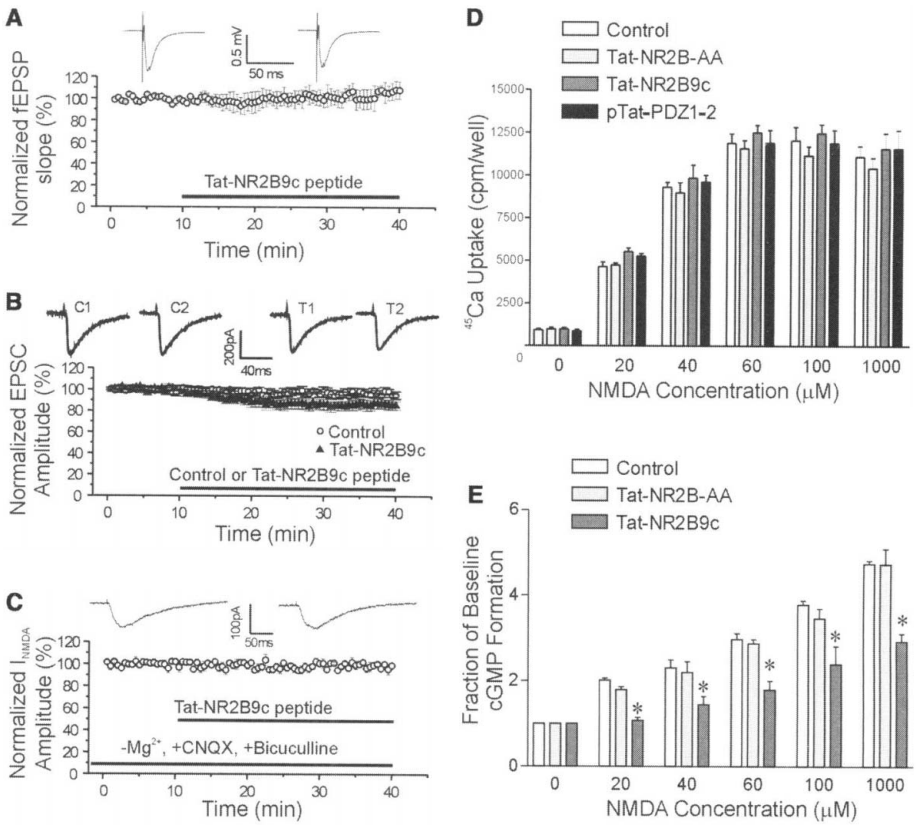

Fig. 2. Neurophysiological effects of Tat peptides (all at 50 nM). (**A**) Effect of Tat-NR2B9c on field EPSCs (fEPSCs) of CA1 neurons in acute hippocampal slices. (**B**) Effect of Tat-NR2B9c or Tat38-48 (control) on whole-cell EPSCs. (**C**) Effect of Tat-NR2B9c on the pharmacologically isolated NMDA component of the EPSC. (**D**) Effect of Tat-peptide pretreatment for 1 hour on NMDA-evoked $^{45}Ca^{2+}$ uptake in cortical cultures. (**E**) Effect of Tat-NR2B9c pretreatment for 1 hour on NMDA-evoked cGMP production in cortical cultures. Asterisk: differences from control and Tat-NR2B-AA at each NMDA concentration (Bonferroni *t* test, $P < 0.01$). Bars in (D) and (E) are means ± SE for 12 cultures in three separate experiments.

Pretreatment with Tat-NR2B9c produced a trend toward improvement in 24-hour neurological scores (fig. S2B). Moreover, the treatment reduced the total cerebral infarction volume by 54.6 ± 11.3% [fig. S2C(i); analysis of variance (ANOVA), $F = 7.289$, $P = 0.0048$]. This was largely accounted for by a 70.7 ± 11.2% reduction in cortical infarction [fig. S2C(ii), ANOVA, $F = 8.354$, $P = 0.0027$], thought to be largely caused by NMDAR-dependent mechanisms.

A stroke treatment with a single-bolus injection would be most therapeutically valuable if effective when given after the onset of ischemia. To evaluate whether Tat peptides could be neuroprotective when applied after insult in vitro, we first exposed cultured cortical neurons to an NMDA challenge (0 to 100 μM) for 1 hour, and then treated these cultures with the Tat peptides (all at 50 nM) described in the pretreatment study (fig. S1). Attenuation of NMDA toxicity in cultures treated with Tat-NR2B9c or pTat-PDZ1-2 was significant relative to cultures treated with control peptides (Fig. 3A).

Finally, we examined whether treatment with Tat-NR2B9c could attenuate ischemic neuronal damage in vivo when applied after stroke onset. Rats were subjected to transient MCAO for 90 min as before, and intravenous saline or Tat-peptide bolus (Tat-NR2B9c or Tat-NR2B-AA; 3 nmol/g) was injected 1 hour after MCAO onset (Fig. 3C, inset). Infarction volume and neurological outcome measurements were performed at times identical to the pretreatment study. Physiological parameters were monitored throughout the 24-hour experiment and were maintained equivalent between groups (table S2). Animals treated after MCAO with Tat-NR2B9c, but not with Tat-NR2B-AA or saline, exhibited a significant improvement in 24-hour neurological scores (Fig. 3B; ANOVA, $F = 17.25$, $P < 0.0001$). Treatment with Tat-NR2B9c reduced the volume of total cerebral infarction

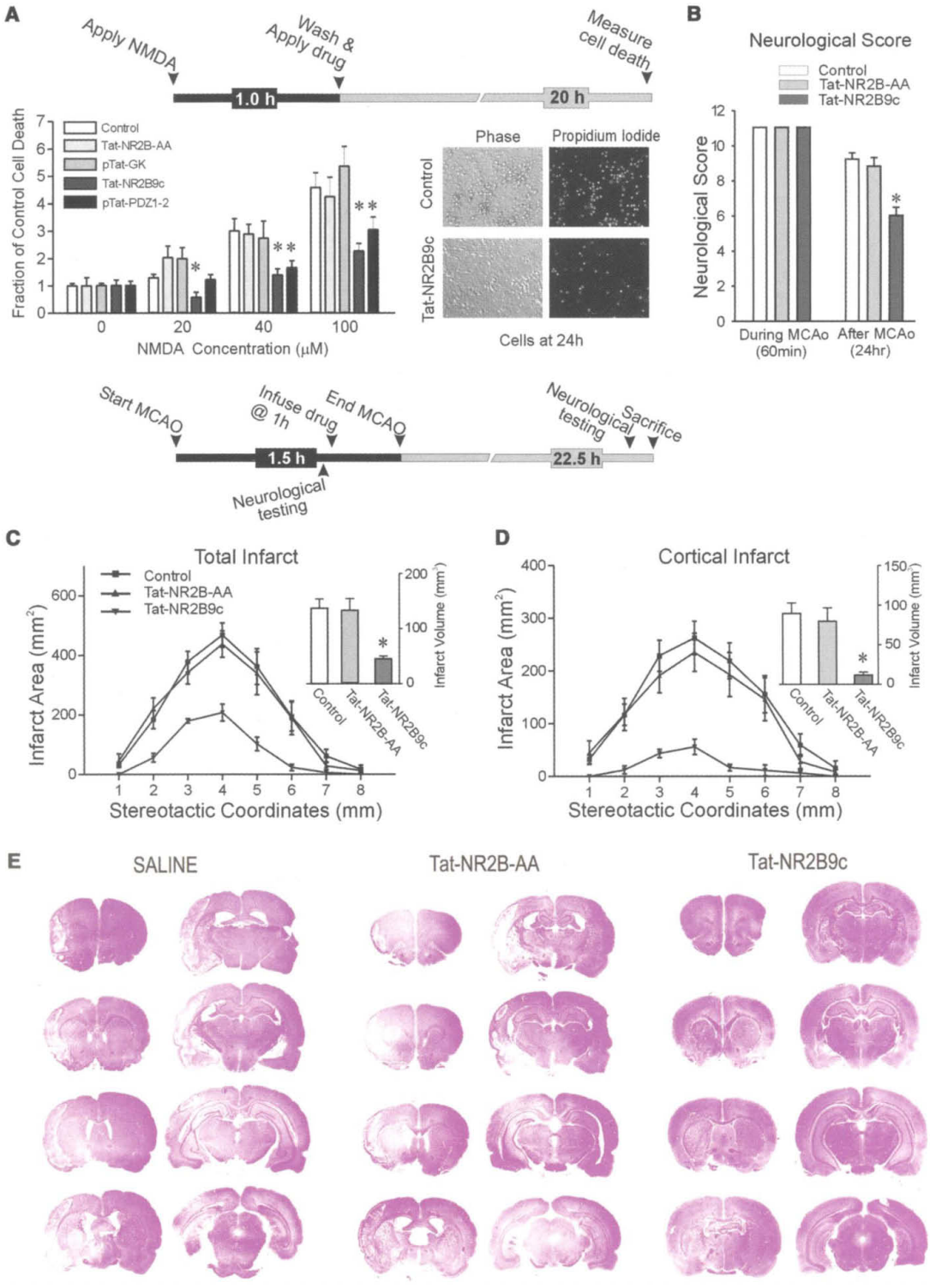

Fig. 3. Neuroprotection after insult by treatment with Tat-NR2B9c in vitro and in vivo. (**A**) Decreased excitotoxicity at 20 hours in cultured cortical neurons treated 1 hour after NMDA application with 50 nM Tat-NR2B9c or pTat-PDZ1-2. Bars indicate means ± SE for 12 cultures in three separate experiments. Asterisk: differences from control, Tat-NR2B-AA and pTat-GK (*13*) at each NMDA concentration (Bonferroni *t* test, $P < 0.005$). (Right) Representative phase contrast and propidium iodide fluorescence images of treated and control cultures 20 hours after challenge with 100 μM NMDA. (**B**) Composite neurological scores (see text) during and 24 hours after MCAO. Asterisk: difference from control and Tat-NR2B-AA (ANOVA; $F = 17.25$, $P < 0.0001$). (**C** and **D**) Treatment with Tat-NR2B9c (3 nmol/g, 9 animals) but not mutated Tat-NR2B-AA (8 animals) or saline controls (10 rats) significantly reduced (C) total infarct area and volume (inset) (ANOVA; $F = 12.0$, $P < 0.0005$) and (D) cortical infarct area and volume (inset) (ANOVA; $F = 12.64$, $P = 0.0001$), measured 24 hours after transient MCAO. Symbols and bars indicate means ± SE. (**E**) Representative appearance of hematoxylin and eosin–stained rat brain sections from each treatment group.

by 67.0 ± 3.7% (Fig. 3C; ANOVA, $F = 11.99$, $P = 0.0002$). Similar to the pretreatment study, this reduction was accounted for by an 87.0 ± 4.4% reduction in cortical infarction volume (Fig. 3, D and E; ANOVA, $F = 12.64$, $P < 0.0001$).

Our results show that introducing into cells an exogenous peptide containing the COOH-terminal nine amino acids of the NR2B NMDAR subunit has profound effects on signaling pathways downstream of NMDAR activation, on in vitro excitotoxicity, and on in vivo ischemic brain damage. The effects of this peptide are lost by mutating amino acids that are essential for mediating PDZ binding to PSD-95. Interfering with the interaction between NMDARs and PSD-95 may interrupt signaling downstream from NMDARs that leads to neuronal death. Because this occurs without affecting NMDAR activity, adverse consequences of blocking NMDARs are not expected. Efficacy after the insult onset suggests targeting of the NMDAR–PSD-95 interaction as a practical future strategy for treating stroke. It is probable that a similar approach could be used to modulate signals mediated by protein-protein interactions that lead to other human diseases.

References and Notes

1. T. Pawson, J. D. Scott, *Science* **278**, 2075 (1997).
2. M. Sheng, *Proc. Natl. Acad. Sci. U.S.A.* **98**, 7058 (2001).
3. H. C. Kornau, L. T. Schenker, M. B. Kennedy, P. H. Seeburg, *Science* **269**, 1737 (1995).
4. J. E. Brenman *et al.*, *Cell* **84**, 757 (1996).
5. V. L. Dawson, T. M. Dawson, E. D. London, D. S. Bredt, S. H. Snyder, *Proc. Natl. Acad. Sci. U.S.A.* **88**, 6368 (1991).
6. M. Migaud *et al.*, *Nature* **396**, 433 (1998).
7. R. Sattler *et al.*, *Science* **284**, 1845 (1999).
8. R. P. Simon, J. H. Swan, B. S. Meldrum, *Science* **226**, 850 (1984).
9. A. S. Fix *et al.*, *Exp. Neurol.* **123**, 204 (1993).
10. S. M. Davis *et al.*, *Stroke* **31**, 347 (2000).
11. G. F. Morris *et al.*, *J. Neurosurg.* **91**, 737 (1999).
12. S. R. Schwarze, A. Ho, A. Vocero-Akbani, S. F. Dowdy, *Science* **285**, 1569 (1999).
13. See supporting data on *Science* Online.
14. D. A. Mann, A. D. Frankel, *EMBO J.* **10**, 1733 (1991).
15. Total EPSCs were recorded under conditions in which they are mediated by AMPARs (holding membrane potential of −60 mV, 2 mM extracellular Mg^{2+}).
16. Ratios of peak $[Ca^{2+}]_i$ and rate of rise of $[Ca^{2+}]_i$ before and after Tat-NR2B9c application were 1.03 ± 0.03 and 0.99 ± 0.04, respectively (n = 11 neurons).
17. R. Sattler, M. P. Charlton, M. Hafner, M. Tymianski, *J. Neurochem.* **71**, 2349 (1998).
18. R. Sattler, Z. Xiong, W. Y. Lu, J. F. MacDonald, M. Tymianski, *J. Neurosci.* **20**, 22 (2000).
19. S. R. Jaffrey, S. H. Snyder, *Annu. Rev. Cell Dev. Biol.* **11**, 417 (1995).
20. Tat-NR2B9c-dansyl fluorescence was visualized in all other brain areas examined (hippocampus, striatum).
21. Tat-NR2B9c-dansyl fluorescence was detectable in brain vessels and all brain regions examined in 250-g Sprague-Dawley rats 1 hour after intravenous injection (3 nmol/g).
22. E. Z. Longa, P. R. Weinstein, S. Carlson, R. Cummins, *Stroke* **20**, 84 (1989).
23. L. Belayev, O. F. Alonso, R. Busto, W. Zhao, M. D. Ginsberg, *Stroke* **27**, 1616 (1996).
24. J. B. Bederson *et al.*, *Stroke* **17**, 472 (1986).
25. M. De Ryck, J. van Reempts, M. Borgers, A. Wauquier, P. A. Janssen, *Stroke* **20**, 1383 (1989).
26. Supported by NIH grant NS 39060 (M.T.) and the Canadian Stroke Network (M.T., M.W.S., Y.T.W., J.G.). M.A. is a fellow of the Ontario Heart and Stroke Foundation. M.T. is a Canadian Institutes of Health Research Clinician-Scientist. Y.T.W. is the holder of the Heart Stroke Foundation of British Columbia and Yukon Chair in Stroke Research at the University of British Columbia. We thank J. F. MacDonald, L.-Y. Wang, M. Goldberg, and J. MacManus for a critical review of the manuscript, and L. Teves and Y. Li for technical assistance.

Supporting Online Material

www.sciencemag.org/cgi/content/full/298/5594/846/DC1
Materials and Methods
Supplemental Online Text
Tables S1 and S2
Figs. S1 and S2

15 April 2002; accepted 3 September 2002

Cancer Regression and Autoimmunity in Patients After Clonal Repopulation with Antitumor Lymphocytes

Mark E. Dudley,[1] John R. Wunderlich,[1] Paul F. Robbins,[1] James C. Yang,[1] Patrick Hwu,[1] Douglas J. Schwartzentruber,[1] Suzanne L. Topalian,[1] Richard Sherry,[1] Nicholas P. Restifo,[1] Amy M. Hubicki,[1] Michael R. Robinson,[2] Mark Raffeld,[3] Paul Duray,[3] Claudia A. Seipp,[1] Linda Rogers-Freezer,[1] Kathleen E. Morton,[1] Sharon A. Mavroukakis,[1] Donald E. White,[1] Steven A. Rosenberg[1]*

We report here the adoptive transfer, to patients with metastatic melanoma, of highly selected tumor-reactive T cells directed against overexpressed self-derived differentiation antigens after a nonmyeloablative conditioning regimen. This approach resulted in the persistent clonal repopulation of T cells in those cancer patients, with the transferred cells proliferating in vivo, displaying functional activity, and trafficking to tumor sites. This led to regression of the patients' metastatic melanoma as well as to the onset of autoimmune melanocyte destruction. This approach presents new possibilities for the treatment of patients with cancer as well as patients with human immunodeficiency virus–related acquired immunodeficiency syndrome and other infectious diseases.

Immunotherapy of patients with cancer requires the in vivo generation of large numbers of highly reactive antitumor lymphocytes that are not restrained by normal tolerance mechanisms and are capable of sustaining immunity against solid tumors. Immunization of melanoma patients with cancer antigens can increase the number of circulating $CD8^+$ cytotoxic T lymphocyte precursor cells (pCTLs), but to date this has not correlated with clinical tumor regression, suggesting a defect in function or activation of the pCTLs (*1*).

Adoptive cell transfer therapies provide the opportunity to overcome tolerogenic mechanisms by enabling the selection and activation of highly reactive T cell subpopulations and by manipulation of the host environment into which the T cells are introduced. However, prior clinical trials, including the transfer of highly active antitumor T cell clones, failed to demonstrate engraftment and persistence of the transferred cells (*2–5*). Lymphodepletion can have a marked effect on the efficacy of T cell transfer therapy in murine models (*6–9*) and may depend on the destruction of regulatory cells, disruption of homeostatic T cell regulation, or abrogation of other normal tolerogenic mechanisms.

To determine whether prior lymphodepletion might improve the persistence and function of adoptively transferred cells, 13 HLA-$A2^+$ patients with metastatic melanoma received immunodepleting chemotherapy with cyclophosphamide and fludarabine for 7 days before the adoptive transfer of highly selected tumor-reactive T cells and high-dose interleukin-2 (IL-2) therapy (*10*) (Table 1). These patients all had progressive disease refractory to standard therapies, including high-dose IL-2, and eight patients also had progressive disease despite aggressive chemotherapy. The patients received an average of 7.8×10^{10} cells (range, 2.3×10^{10} to 13.7×10^{10}) and an average of nine doses of IL-2 (range, 5 to 12 doses). The T cells used for treatment were derived from tumor-infiltrating lymphocytes (TILs) and were rapidly expanded in vitro (*11*). All cultures were highly reactive when stimulated with an HLA-$A2^+$ melanoma or an autologous melanoma cell line (Table 1 and table S1).

Six of the 13 patients had objective clinical responses to treatment and four others demonstrated mixed responses, with significant shrinkage of one or more metastatic deposits (*11*). Objective tumor regression was seen in the lung, liver, lymph nodes, and intraperitoneal masses and at cutaneous and subcutaneous sites. Five patients, all with evidence of concomitant cancer regression, demonstrated signs of autoimmune melanocyte destruction, including four patients with vitiligo and one patient with anterior uveitis (Table 1). All patients recovered from treatment with absolute neutrophil counts greater than 500/mm^3 by day 11 after T cell infusion but with slower recovery of $CD4^+$ cells, as expected after fludarabine therapy (*12*).

To investigate the function and fate of the transferred T cell populations, T cell receptor (TCR) expression was examined using a pan-

[1]Surgery Branch, National Cancer Institute; [2]National Eye Institute; [3]Laboratory of Pathology, National Cancer Institute; National Institutes of Health, Bethesda, MD 20902, USA.

*To whom correspondence should be addressed. E-mail: SAR@nih.gov